ISSN (Print) 1226-1750
ISSN (Online) 2233-6656
Journal of Magnetics 23(4), 624-631 (2018) https://doi.org/10.4283/JMAG.2018.23.4.624

A Study on Image Distortion by Contrast Agent Concentration according to 1.5T and 3.0T in Diffusion Weighted Image

Yong Soo Han[1,6], Ki Chang Nam[2], Hyung Shin Park[3], Sun Yeob Lee[4], Cheol Soo Park[4], Ho Beom Lee[5,6], and Sung Min Kim[6]*

[1]*Department of Radiology, Dongguk University Ilsan Medical Center, Goyang 10326, Republic of Korea*
[2]*Department of Medical Engineering, Dongguk University College of Medicine, Goyang 10326, Republic of Korea*
[3]*Department of Health Science, Far East University, Chung-cheong 27601, Republic of Korea*
[4]*Department of Radiological Science, Hallym Polytechnic University, Chuncheon 24210, Republic of Korea*
[5]*Department of Radiology, Asan medical center, Seoul 05505, Republic of Korea*
[6]*Department of Medical Device Industry, Dongguk University, Goyang 10326, Republic of Korea*

(Received 26 November 2018, Received in final form 19 December 2018, Accepted 19 December 2018)

The correlation between the readout segment and the GeneRalized Auto Calibrating Partial Parallel Acquisition (GRAPPA) acceleration factor in the Read out segmentation of long variable echo-trains Diffusion Weighted Image (RESOLVE DWI) after enhancement was analyzed to investigate the effects of the signal intensity and the image distortion on the difference of the main field and contrast agent concentration. Twenty - four phantoms were prepared for each concentration of contrast agent, and signal intensity and image distortion were evaluated. At 1.5T and 3.0T, images were acquired using Readout segment, GRAPPA acceleration factor and echo spacing parameters, and Roundness (%) was measured using Regions Of Interest Contours. As the readout segment increased, signal strength and image distortion decreased. As the GRAPPA acceleration factor increased, signal strength increased and image distortion decreased. In RESOLVE DWI, it is helpful to minimize the distortions and artifacts caused by the signal intensity detection in the contrast agent phantom experiment and confirm the correlation between the readout segment and the GRAPPA acceleration factor depending on the main field, thereby making it possible to produce images with high diagnostic value.

Keywords : Diffusion Weighted Image, read out segmentation of long variable echo-trains (RESOLVE), parallel imaging, gadolinium contrast, image distortion

1. Introduction

Diffusion Weighted Imaging (DWI) is important for evaluation of diagnosis and treatment, such as primary cerebral infarction, brain tumor diagnosis, and post-operative follow-up [1-3]. Recently, it has also been used for diagnosis of abdominal pain, pancreas, prostate, gynecological diseases and rectal cancer, and it is also used for differentiating breast diseases and muscle-skeletal tumors [4-9].

Water molecules present between normal cells spread smoothly because of the large diffusion space. But Water molecules that exist between abnormal cells such as cerebrovascular diseases and tumor cells decrease diffusion movement. In normal tissues, diffusion is well established and the diffusion coefficient is increased. However, in case of cerebrovascular disease, the oxygen supply from the blood is decreased, and intracellular edema occurs. The extracellular water molecule diffusion movement is limited and diffusion coefficient becomes small. In addition, the dissociation of water molecules between tumor cells is reduced by the undifferentiated cell tissue of malignant tumor, and the diffusion coefficient is decreased [10-12].

The principle of DWI uses the Motion Proving Gradient (MPG), which is a diffusion gradient magnetic field with strong intensity before and after refocusing pulse after excitation pulse. It is the image using the signal difference of the in-phasing spins relatively due to the decrease of the signal of the de-phasing spins and the disturbance of the diffusion motion. The intensity of the diffusion gradient magnetic field is represented by b-value, and the

*Corresponding author: Tel: +82-31-961-7832
Fax: +82-31-961-7832, e-mail: sungmin2009@gmail.com

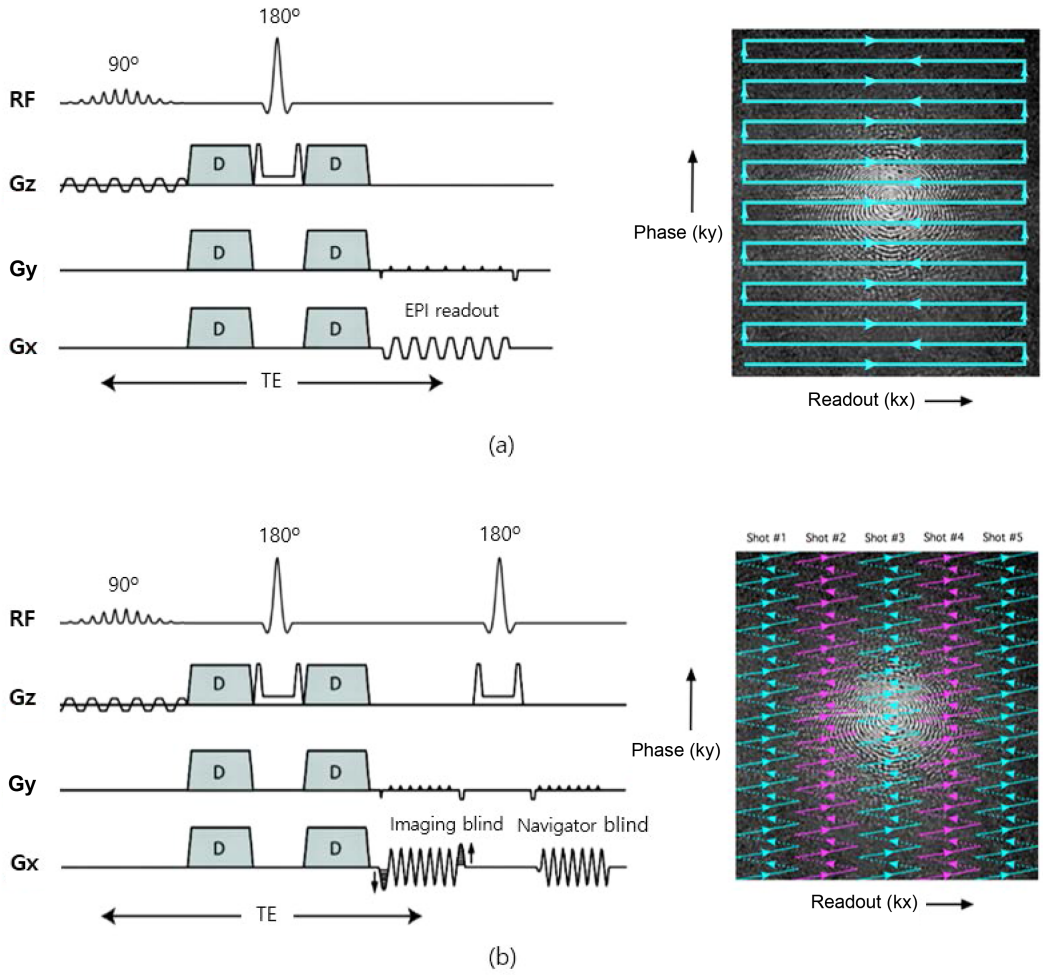

Fig. 1. (Color online) (a) Single shot echo-planar imaging (SS-EPI), (b) Readout segmentation of long variable echo-trains (RESOLVE).

signal intensity of the DWI decreases as the diffusion coefficient (unit : mm^2/sec) of the tissue and gradient are larger. And In order to make the difference of the diffusion motion occurring in the microscopic unit as the difference of the image signal, the signal is collected using the Echo Planner Image (EPI) technique having the shortest image acquisition time [13].

EPI has a single-shot echo planar image (SS-EPI) (Fig. 1a) and a 2D navigator-based reacquisition readout segment (RS-EPI) (Fig. 1b). The SS-EPI collects all the signals that make up the image with a single excitation pulse. Therefore, k-space is filled with a signal without correction of the phase error of the image section due to the application of the phase encoding gradient. All the signals collected at high speed are phase error, and the phase errors of each echo are getting bigger by the acquisition of consecutive signals. In addition, the phase error in the slice selection direction in the slice selection gradient affects image acquisition. As the slice selection gradient moves away from the center of the k-space, the image distortion and artifact increase along the slice encoding gradient direction. RS-EPI reduces echo train length (ETL) and reduces echo spacing (ESP) to prevent magnetization susceptibility and artifacts from T2 * decay. Since the echo spacing is reduced by sub-dividing the segmented k-space in the segmentation direction, the time to fill the k-space in the phase encoding direction can be reduced [14]. The 2D navigator technology uses two k-spaces to receive the bipolar readout, and corrects the collected k-space data by direct inverse filtering.

Parallel imaging (PI) technique uses fewer signals in the k-space. The insufficient information reconstructs the image using the sensitivity information of the coils arranged in the phase direction. And the position and sensitivity of the receiving coil are used for spatial positioning of the MR signal [15]. GeneRalized Auto Calibrating Partial Parallel Acquisition (GRAPPA) is a PI technique using Auto Calibrating Reconstruction for Cartesian Imaging

(ARC) of the k-space Frequency domain [16].

Read out segmentation of long variable echo-trains (RESOLVE) can acquire images by minimizing high resolution and distortion using PI and RS-EPI [17].

MR contrast agents are used to enhance the characterization of tissues by increasing the difference in contrast between normal and diseased tissues. DWI is not used for contrast enhancement but requires a delay of 10-30 minutes after hepatocellular carcinoma (HCC) to obtain hepato biliary delayed phase images. For the efficiency of the test, the DWI test is performed after contrast medium administration [18, 19]. Although DWI is known to have no clinical effect, it is believed that Gadolinium (Gd) with the paramagnetic effect of atomic number 64 changes the relaxation time of 1H in the body and that the changed energy level will affect the EPI signal intensity do.

In this study, we constructed the MRI contrast agent phantom and evaluated the distortion distortion according to the parameters of Readout segment (Seg.) And GRAPPA acceleration factor (Gf) at 1.5T and 3.0T using various parameters that cause image distortion in RESOLVE DWI.

2. Materials and Methods

2.1. Phantom production

RESOLVE To confirm the image distortion caused by contrast agent concentration in DWI, PRIMOVIST® (181.43 mg) of Gadoxetic acid (Gd-EOB-DTPA) series used to obtain hepatobiliary delayed phase images of hepatocellular carcinoma (HCC)/mL, 0.25 mol/L, Bayer) (Fig. 2). Twenty-four phantoms were prepared by diluting PRIMOVIST® and physiological saline in a 1.4 cm diameter cylindrical syringe with a total volume of 3 mL, ranging from 0.05 mmol/mL to 50 mmol/mL, and image data were analyzed (Table 1).

Fig. 2. (Color online) Twenty-four cylindrical Phantom diluted with Primovist and nomal saline.

2.2. Research method

The instrument used in this experiment was 1.5T Magnetom Avanto (Siemens Medical System, Germany) and

Table 1. Degree of concentration Phantom.

PRIMOVIST® Degree of concentration Phantom							
mmol	Contrast	Saline	Volume (mL)	mmol	Contrast	Saline	Volume (mL)
50	0.6	2.4	3	2	0.024	2.976	3
40	0.48	2.52	3	1	0.012	2.988	3
30	0.36	2.64	3	0.9	0.0108	2.9892	3
20	0.24	2.76	3	0.8	0.0096	2.9904	3
10	0.12	2.88	3	0.7	0.0084	2.9916	3
9	0.108	2.892	3	0.6	0.0072	2.9928	3
8	0.096	2.904	3	0.5	0.006	2.994	3
7	0.084	2.916	3	0.4	0.0048	2.9952	3
6	0.072	2.928	3	0.3	0.0036	2.9964	3
5	0.06	2.94	3	0.2	0.0024	2.9976	3
4	0.048	2.952	3	0.1	0.0012	2.9988	3
3	0.036	2.964	3	0.05	0.0006	2.9994	3

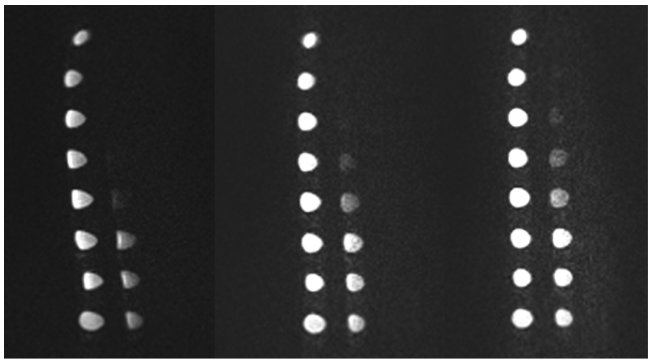

(a) (b) (c)

Fig. 3. (Color online) Distorted image due to correlation between Readout segment and GRAPPA acceleration factor at 3T. (a) Image for GRAPPA acceleration factor 2 for Readout segment 4, (b) Image for GRAPPA acceleration factor 3 for Readout segment 4, (c) Image for GRAPPA acceleration factor 4 for Readout segment 4.

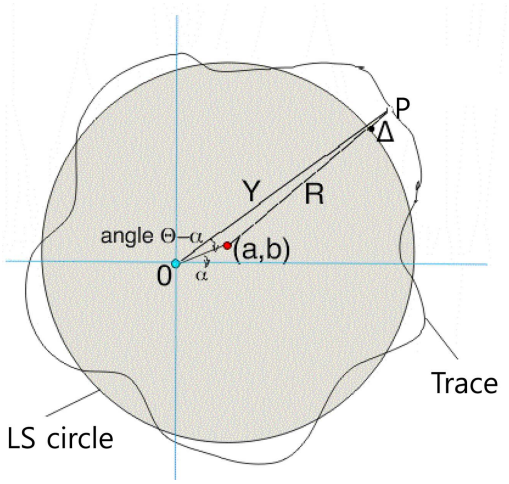

Fig. 4. (Color online) Roundness (%) measurements.

3T Magnetom Skyra (Siemens Medical System, Germany). The coil used for signal acquisition is respectively 12 Channel Head coil, 20 Channel Head and Neck coil. The parameters of RESOLVE DWI are TR: 9000 ms, TE: 123 ms, ESP 0. ms, average 1, b-value 1000, FOV 220 mm, matrix 182 × 182, slice thickness 3 mm, gap 0.3 mm. The experimental method is Seg. (3, 5, 7) and G.f (2, 3, 4) were cross-tested five times. seg. 7 and G.f 4 condition was tested by changing the ESP (0.34 ms, 0.44 ms, 0.58 ms, 0.70 ms, 0.84 ms, 0.94 ms) (Fig. 3). The reference scan mode is EPI/separate and the filter is Prescan Nomalize

2.3. Comparative analysis

In the RESOLVE DWI, Icy program (ver.1.9.9.0, http://icy.bioimageanalysis.org) was used to evaluate the image distortion according to the variables of Seg. And G.f. Roundness (%) was derived using ROI Contours protocol, which can extract Regions Of Interest (ROI), to quantitatively measure the geometrical contour due to distortion due to difference in magnetization susceptibility (Fig. 4). Roundness (%) is the standardized percentage expressed as a percentage (100 % for circles or spheres) between the circles and the circles circumscribed by the ISO 1001 standard. This measure is similar to the Sphericity (defined by H. Wadell in 1935) measurement, but is much more sensitive to small shape deformations and the equations are shown in Eq. (1).

$$\hat{\Delta} = R_i - \hat{R} - \hat{a}\cos\theta_i - \hat{b}\sin\theta_i \tag{1}$$

$$\hat{R} = \frac{1}{N}\sum_{i=1}^{N} R_i \tag{1-1}$$

Table 2. Roundness (%) data analysis results of 1.5T.

	seg3			seg5			seg7		
mmol	G.f2	G.f3	G.f4	G.f2	G.f3	G.f4	G.f2	G.f3	G.f4
1	68.05	68.41	68.41	65.08	70.92	65.59	68.06	70.92	70.92
0.9	65.69	68.41	68.41	65.08	68.06	70.71	68.05	68.05	70.92
0.8	70.71	68.41	68.41	68.05	68.05	68.05	70.92	70.92	70.92
0.7	68.41	70.71	68.41	65.08	70.92	70.92	68.06	70.92	70.92
0.6	65.69	68.05	70.92	65.08	65.08	68.05	65.08	70.92	68.05
0.5	68.41	68.41	68.05	65.08	68.05	68.05	65.08	68.05	70.92
0.4	68.41	65.08	68.41	68.06	68.05	70.92	68.06	70.92	68.05
0.3	70.71	68.05	68.41	68.06	68.05	68.05	65.08	68.05	68.06
0.2	65.69	70.71	68.41	65.08	65.08	68.05	70.92	70.92	70.92
0.1	70.71	70.71	70.71	65.08	65.08	70.92	68.05	68.05	70.92
0.05	68.41	68.41	68.41	68.05	68.05	70.92	65.08	68.05	70.92
Avg.	68.26	68.67	68.81	66.16	67.76	69.11	67.49	69.61	70.14

$$\hat{a} = \frac{2}{N}\sum_{i=1}^{N} R_i \cos\theta_i \quad (1\text{-}2)$$

$$\hat{b} = \frac{2}{N}\sum_{i=1}^{N} R_i \sin\theta_i \quad (1\text{-}3)$$

Statistical analysis was performed using correlation analysis (Pearson correlation coefficient, SPSS version 22.0, IBM Co., Armonk, NY, USA) p value of less than 0.05 was considered significant.

3. Results

After using Gd contrast agent, 1.5T and 3.0T RESOLVE DWI were used. And G.f are the results of the data analysis on the image distortions obtained.

RESOLVE DWI signal intensity by 1.5T contrast medium concentration Seg. (3, 5, 7), G.f (2, 3, 4) Signals were measured from 1 mmol to 0.05 mmol in all experimental conditions (Table 2). In the correlation analysis for each factor, Seg. And signal intensity showed strong negative correlation (–.912**) and not significant with Roundness (%). There was a strong positive correlation (.901**) between G.f and Roundness (%), but not with signal intensity (Fig. 5, Table 3).

Table 3. Roundness (%) correlation analysis result of 1.5T.

		SI	Roundness
Segment	Pearson Correlation Sig. (2-tailed)	–.912** 0	0.127 0.748
GRAPPA	Pearson Correlation Sig. (2-tailed)	0.107 0.624	.901** 0

**Correlation is significant at 0.01 (two-tailed) level.

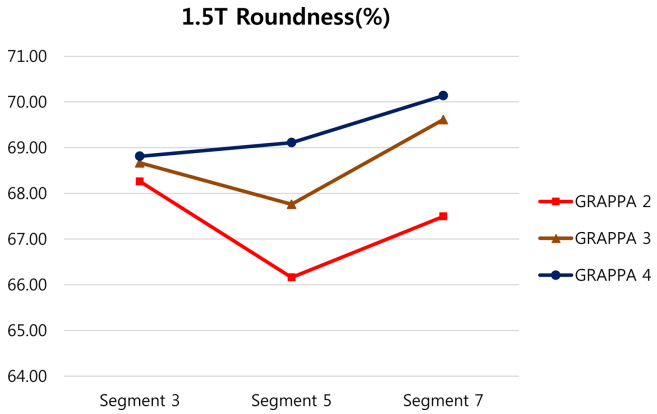

Fig. 5. (Color online) Roundness (%) by segment according to GRAPPA (1.5T).

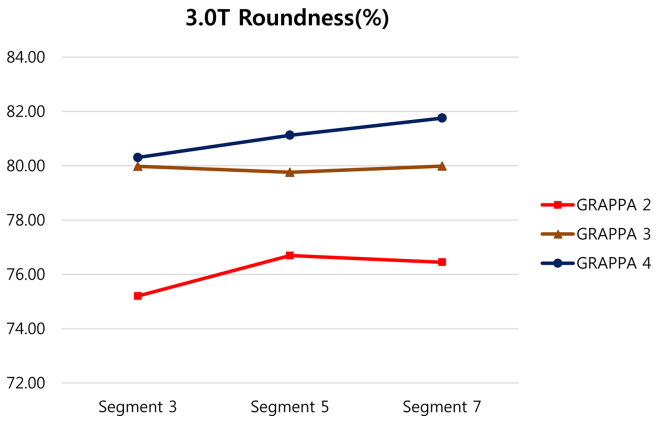

Fig. 6. (Color online) Roundness (%) by segment according to GRAPPA (3.0T).

Table 4. Roundness (%) data analysis results of 3.0T.

	seg.3			seg.5			seg.7		
mmol	G.f2	G.f3	G.f4	G.f2	G.f3	G.f4	G.f2	G.f3	G.f4
3		78.18	82.95		78.12	79.01	69.83	83.53	81.97
2	77.65	80.81	80.63	74.71	63.55	70.22	75.28	83.46	83.16
1	75.56	80.03	84.07	77.78	79.32	78.11	78.30	82.03	82.80
0.9	79.77	80.60	82.97	75.16	83.87	84.62	78.74	79.62	79.96
0.8	67.27	77.76	78.49	73.76	77.58	78.72	73.25	73.82	73.50
0.7	72.14	74.22	72.46	72.96	77.47	80.59	74.02	78.13	83.38
0.6	80.22	80.29	82.92	80.57	83.29	84.43	77.61	76.84	84.59
0.5	76.43	78.42	74.24	75.11	81.96	84.51	76.38	78.65	81.41
0.4	74.87	80.95	78.01	77.31	80.97	83.48	78.85	79.67	82.51
0.3	75.66	83.70	82.81	77.76	84.43	82.08	81.35	85.85	84.24
0.2	75.11	83.78	79.84	81.90	82.11	78.85	79.29	82.13	82.94
0.1	72.01	83.36	83.34	75.84	80.56	83.98	75.83	76.38	80.59
0.05	75.75	77.60	81.25	77.44	83.60	86.02	75.07	79.69	81.74
Avg.	75.20	79.98	80.30	76.69	79.76	81.12	76.45	79.98	81.75

Table 5. Roundness (%) correlation analysis result of 3.0T.

		SI	Roundness
Segment	Pearson Correlation Sig. (2-tailed)	–.969** 0	0.111 0.732
GRAPPA	Pearson Correlation Sig. (2-tailed)	0.141 0.675	.908** 0

**Correlation is significant at 0.01 (two-tailed) level.

Table 6. Data analysis results by echo spacing (1.5T).

echo spacing (mmsc)	Signal Intensity	Standard Deviation	Contrast	Roundness (%)	Homogeneity
0.44	67.47	52.17	1433.56	69.43	0.05
0.58	70.20	56.62	1608.55	70.18	0.06
0.70	66.35	55.09	1457.37	68.74	0.06
0.84	64.67	53.64	1370.27	69.84	0.07
0.94	59.93	52.70	1269.27	69.40	0.07

RESOLVE DWI signal intensity by 3.0T contrast medium concentration Seg. (3, 5, 7), G.f2 was measured from 2 mmol to 0.05 mmol, Seg. (3, 5, 7), G.f (3, 4) signals were measured from 3 to 0.05 mmol (Table 4).

In the correlation analysis, Seg. And signal intensity showed strong negative correlation (–.969**) and not significant with Roundness (%). There was a strong positive correlation (.908**) between G.f and Roundness (%), but not with signal intensity (Fig. 6, Table 5).

At 1.5T, the best evaluation of the distortion according to the ESP difference in Seg.7 and G.f4, which has the best distortion degree, was the best at 70.18 % at 0.58 msec, which was the highest signal intensity at 70.20 (Table 6).

4. Discussion

To obtain hepatobiliary delayed phase images of hepatocellular carcinoma (HCC), a delay of 20 minutes or longer should be performed after contrast injection. In terms of the efficiency of the examination time, T2 and DWI excluding T1 are examined after contrast injection. Michael *et al.* [20] used 3D fluid-attenuated in ersion recovery (T2-3D) technique to assess the effectiveness of vestibular stimulation in patients with acute vestibular syndrome after contrast enhancement. In DWI, various studies such as influence of signal intensity and distortion due to magnetization susceptibility have been carried out.

Because DWI acquires signals using EPI, which is a super high-speed technique, it is affected by difference in magnetization sensitivity, recursive transition, uniformity of runner field [21]. The larger the b-value, the greater the diffusion effect, and thus the larger the b-value gradient is applied. The effect of T2 effect is shown by increasing TE. To solve this problem, a method for reducing TE should be selected. RESOLVE DWI increases TE and ESP by increasing Seg. and shortens TE by using parallel imaging factor. In addition, when the Gd contrast agent is introduced into the human body, the difference in the susceptibility becomes so great that the distortion of the image becomes larger, which greatly affects anatomical and pathological image evaluation. Jeong *et al.* [22] have reported quantitative data analysis of the signal intensity changes in SS-EPI DWI with Gd contrast agent, but there is no analysis of RS-EPI and PI. Han *et al.* [23] studied the occurrence of Nyquist Ghost Artifact (NGA) according to Seg. and G.f in RESOLVE DWI, but failed to propose a solution to image distortion. In addition, Tan *et al.* [24] studied the reduction of distortion according to the high gradient slew-rates in EPI, but failed to propose the degree of distortion due to the main field difference at the same gradient slew-rates.

RESOLVE DWI uses both PI and RS-EPI to acquire images by minimizing the effects of distortion and artifacts caused by differences in resolution and magnetization susceptibility. The PI technique is a technique in which the position and sensitivity of the receiving coil are used to determine the spatial position of the MR signal. This additional information on the coil has the advantage of reducing the image acquisition time by reducing the number of phase-encoding in image acquisition, but there is a disadvantage that SNR decreases and artifact increases as G.f increases.

In this study, we confirmed the difference of image distortion according to the concentration of contrast agent in RESOLVE DWI. In addition, image distortion was

evaluated by 1.5T and 3.0T difference at the same gradient field strength of 45 mT/m and gradient slew rates of 200 T/m/s.

The 1.5T image distortion measurement showed an average increase of 0.5 % when applying G.f2, G.f3, and G.f4 in Seg.3, and an average increase of 2.0 % when applying G.f2, G.f3, and G.f4 in Seg.5. Also Seg.7 showed an average increase of 1.2 % when G.f2, G.f3, and G.f4 were applied. As G.f increases, the image distortion is smaller, but Seg. No significant than was confirmed. The 3.0T image distortion measurement showed an average increase of 3.2 % when applying G.f2, G.f3, and G.f4 in Seg.3, and an average increase of 2.8 % when applying G.f2, G.f3, and G.f4 in Seg.5. Also Seg.7 showed an average increase of 3.4 % when G.f2, G.f3, and G.f4 were applied. As G.f increases, the image distortion is smaller, but Seg. No significant than was confirmed.

The roundness (%) of 1.5T and 3.0T were 68.45 % and 79.03 %, respectively. The difference was 3.0T, 13.4 % higher. This indicates that the artifacts due to the difference in magnetization sensitivity appear more in the high magnetic field, but in the case of the limited image distortion only, the high magnetic field is superior.

Roundness (%) at 1.5T was the best at Seg.7 and G.f4 conditions. As a result of comparing the distortion measurement according to the ESP, the average difference of 2 % was not large. However, the signal intensity was the largest at 0.58 msec to 70.204, and the difference was 15.9 % from 0.94 msec to 59.932 msec.

In this study, Seg. TR, and TE were automatically optimized when parameters such as setting value and ESP were changed, so that no experimental results could be obtained due to a single parameter change. There was a limitation in that it was not able to accurately evaluate the motion that might occur in actual clinical practice, such as the motion of the airway and breathing. Also, we could not obtain the results according to the difference of gradient slew rates of 1.5T and 3.0T equipment.

5. Conclusions

In RESOLVE DWI, the influence on signal strength, artifacts and image distortion should be minimized when determining the parameters after contrast enhancement. Experiment result, Signal strength and image distortion decreased with increasing Seg. As G.f increased, signal intensity increased and image distortion decreased. As the Seg. Increases, the ETL becomes shorter, the TE becomes smaller, and the smaller the ESP is set, the more the magnetization sensitivity and the artifact due to T2 * decay are reduced, but the image acquisition time is increased. However, as G.f increases, the time required to acquire a signal in the K-space in the phase coding direction becomes shorter and the image acquisition time decreases.

By confirming the relationship between Seg., G.f and ESP according to the magnetic field, this study will help to make the image with high diagnostic value in parameter determination.

References

[1] W. Hacke, G. Albers, Y. AI-Rawi, J. Bogousslavsky, A. Davalos, M. Eliasziw, M. Fischer, A. Furlan, M. Kaste, K. R. Lees, M. Soehngen, and S. Warach, Stroke. **36**, 66 (2005).
[2] M. P. James, J. Reza, P. N. Thomas, and J. F. Allan, Radiology **229**, 347 (2003).
[3] The National Institute of Neurological Disorders ancl Stroke rt-PA Stroke Study Group, N Engl. J Med. **333**, 1581 (1995).
[4] J. H. M. Chan, E. Y. K. Tsui, S. H. Luk, A. S. L. Fung, M. K. Yuen, M. L. Szeto, Y. K. Cheung, and K. P. C. Wong, Abdominal Imaging **26**, 161 (2001).
[5] E. Squillaci, G. Manenti, M. Cova, M. Di-Roma, R. Miano, G. Palmieri, and G. Simonetti, Anticancer Research **24**, 4175 (2004).
[6] D. M. Koh, G. Brown, A. M. Riddell, E. Scur, D. J. Collins, S. D. Allen, I. Chau, D. Cunningham, N. M. deSouza, M. O. Leach, and J. E. Husband, European Radiology **18**, 903 (2008).
[7] M. Eiber, A.J. Beer, K. Holzapfel, R. Tauber, C. Ganter, G. Weirich, B. J. Krause, E. J. Rummeny, and J. Gaa, Investigative Radiology **45**, 15 (2010).
[8] C. Marini, C. Iacconi, M. Giannelli, A. Cilotti, M. Moretti, and C. Bartolozzi, European Radiology **17**, 2646 (2007).
[9] X. Xu, J. S. Zhang, L. Ma, Y. Q. Cai, L. Q. Cheng, F. Sun, and X. G. Guo, Chinese Journal of Medical Imaging Technology **6**, 4 (2007).
[10] E. Karaarslan and A. Arslan, Eur. J. Radiol. **65**, 402 (2008).
[11] P. W. Schaefer, W. A. Copen, M. H. Lev, and R. G. Gonzalez, Magn. Reson. Imaging Clin N Am. **14**, 141 (2006).
[12] R. Bammer, Eur. J. Radiol. **45**, 169 (2003).
[13] O. Josephs, R. Deichmann, and R. Turner, NeuroImage. **11**, 543 (2000).
[14] D. A. Porter and R. M. Heidemann, Magn. Reson. Med. **62**, 468 (2009).
[15] S. O. Schoenberg, O. Dietrich, and M. F. Reiser, "Parallel Imaging in Clinical MR Applications" (2007) pp 230.
[16] M. Blaimer, F. Breuer, M. Mueller, R. M. Heidemann, M. A. Griswold, and P. M. Jakob, Top Magn. Reson. Imaging **15**, 226 (2004).
[17] M. A. Griswold, P. M. Jakob, R. M. Heidemann, M. Nit-

tka, V. Jellus, J. Wang, B. Kiefer, and A. Haase, Magnetic Resonance in Medicine **47**, 1202 (2002).
[18] K. Holzapfel, C. Breitwieser, C. Prinz, E. J. Rummeny, and J. Gaa, Radiologe **47**, 536 (2007).
[19] M. K. Seale, O. A. Catalano, S. Saini, P. F. Hahn, and D. V. Sahani, Radiology **29**, 1725 (2009).
[20] E. Michael, M. Charles, H. Julien, G. André, T. Michel, B. Benoit, M. Nicolas, K. Laureline, H. Charlotte, and A. Arnaud, European Radiology (2018) pp 1-10.
[21] J. Y. Chung, Y. Han, Z. H. Cho, and H. Park, MAGMA **25**, 205 (2012).
[22] H. K. Jeong, H. C. Kim, and K. C. Nam, The Institute of Electronics and Information Engineers **55**, 495 (2018).
[23] Y. S. Han, J. Y. Kim, and C. S. Park, Journal of the Korean Magnetics Society **28**, 192 (2018).
[24] E. T. Tan, S. K. Lee, P. T. Weavers, D. Graziani, J. E. Piel, Y. Shu, J. Huston III, M. A. Bernstein, and T. K. F. Foo, Journal of Magnetic Resonance Imaging **44**, 1 (2016).